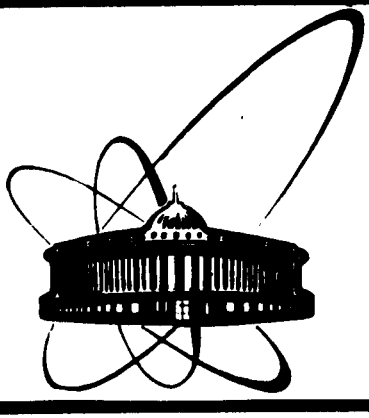

объединенный
институт
ядерных
исследований
дубна

E2-89-349

A.I.Golokhvastov

ACCURATE SCALING ON MULTIPLICITY

Submitted to "Zeitschrift für Physik C"

1989

1. INTRODUCTION

Multiplicity distribution is the probability of production of n particles of a certain type in the inelastic interaction of two particles: $P_n = \sigma_n/\sigma_{in}$. The multiplicity distributions of all charged particles are commonly studied. However, some problems arise in this case: the consideration of protons and π mesons together seems to be incorrect which is especially clear in interactions with nuclei; it is incomprehensible whether leading particles should be included in the disributions (e.g., in a π meson beam); there appears nonuniformity in the distribution due to charge conservation: all odd (or all even) probabilities are equal to zero.

In order not to solve these problems, let us consider the multiplicity distributions of negative hadrons (in fact, π^-mesons) for e^+e^- and PP interactions. They are one-to-one related to the distributions of charged particles: $n_{ch} = 2n_{neg}$ for e^+e^- and

$$n_{ch} = 2n_{neg}+2 \qquad (1)$$

for PP interactions. This equation is also used for $\bar{P}P$ interactions at 546 GeV assuming that the probabilities of changing nucleon (antinucleon) charge at this energy for each multiplicity in PP and $\bar{P}P$ are equal.

Further the multiplicity of negative particles is designated as n.

The multiplicity distributions in e^+e^- annihilation at $\sqrt{s} = 3.35$ GeV [1] (the PLUTO data are taken from the paper of Althoff et al.), in inelastic PP interactions at $P_{lab} = 1.5 \div 2000$ GeV/c [2] and in inelastic $\bar{P}P$ interactions at $\sqrt{s} = 546$ GeV [3] are used for comparison.

2. KNO SCALING

Koba, Nielsen and Olesen have formulated the statement of independence of the multiplicity distribution shape of the energy

of primary particles [4]. This statement was formulated for very high energies, i.e. very large multiplicities, when one can operate with multiplicity distribution as with continuous function. Figure 1a depicts a possible picture of these functions for various primary energies. The area under each curve is equal to unity since it is the sum of all the probabilities: $\int P_n dn = \Sigma P_n = 1$. The average multiplicity ($\langle n \rangle = \Sigma n P_n = \int n P_n dn$) increases with energy.

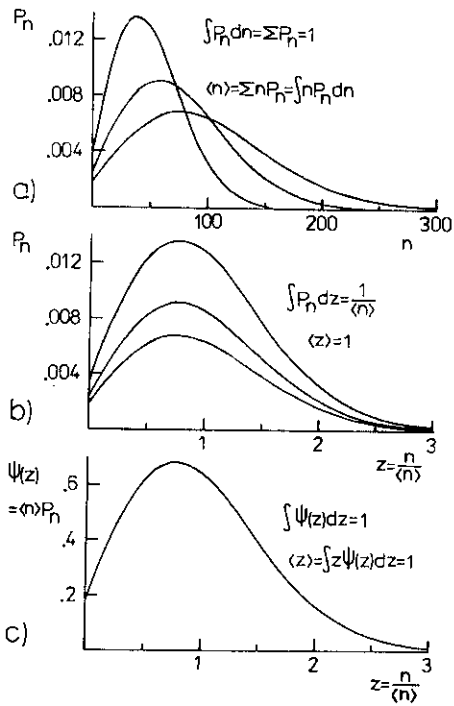

Fig.1. Definition of the concept of similarity for a continuous function (KNO scaling). The normalized functions (a) are similar if after linear compression of each function along the horizontal axis proportionally to any of its horizontal dimensions, e.g. $\langle n \rangle$ (b), and linear stretching along the vertical axis by the same factor (c), they coincide at each point.

Each curve can be compressed along the horizontal axis proportionally to any of its horizontal dimensions, e.g. $\langle n \rangle$ as in fig.1b (either a modal value or width etc.), and stretched along the vertical axis by the same factor in order to make the areas equal again (fig.1c). The statement of KNO scaling consists in that the curves coincide at each point [5]. Figure 1c can be written in the form

$$P_n = 1/\langle n \rangle \, \Psi(n/\langle n \rangle) \, , \qquad (2)$$

where $\Psi(z)$ is an energy-independent function normalized by the conditions

$$\int \Psi(z) dz = 1 \, , \qquad (3)$$

which follows from the equality of the sum of all probabilities to unity, and

$$\int z \Psi(z) dz = 1 \qquad (4)$$

because we compressed the functions P_n until the average value of each function reached unity. Formula (2) imposes no restraints, except (3) and (4), on the shape of the function $\Psi(z)$. It is merely a definition of the concept of similarity for continuous normalized functions.

3. CONTRADICTION

For present-day accelerator energies the function P_n is essentially discrete: the condition $\langle n \rangle \gg 1$ ($\langle n_{ch} \rangle \gg 2$) is not fulfilled. For example, $\langle n \rangle \simeq 2$ at $P_{lab} = 100$ GeV/c and $\langle n \rangle \simeq 5$ at 2000 GeV/c. In this case, irrespective of any physical considerations, formula (2) becomes mathematically incorrect because it contradicts the condition $\Sigma P_n = 1$ as can be shown in fig.2a.

To obtain some multiplicity distribution having a given value of $\langle n \rangle$ from the continuous universal function $\Psi(z)$ in fig.2a, the inverse operation to that in fig.1 should be done, i.e. the scale $z_o = 1/\langle n \rangle$ should be chosen on the z axis. Then the probability P_n

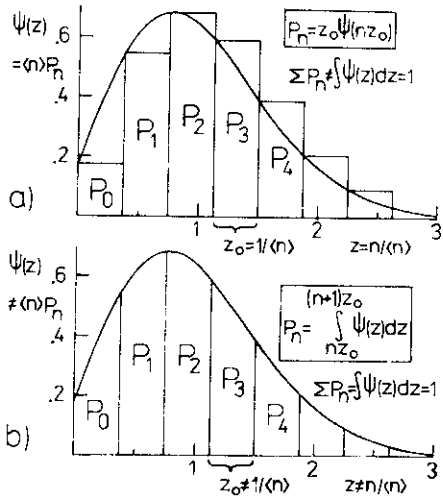

Fig.2. Obtaining of the discrete multiplicity distribution from the continuous normalized universal function $\Psi(z)$; (a)- according to the commonly used recipe $P_n=1/\langle n\rangle\ \Psi(n/\langle n\rangle)$, then $\Sigma P_n \neq 1$; (b)- according to the correct recipe.

is equal to the area of the rectangle which touches the curve $\Psi(z)$ by its left vertex at the point $z= nz_0= n/\langle n\rangle$. The height of the rectangle is $\Psi(n/\langle n\rangle)= \langle n\rangle P_n$ and its base is $1/\langle n\rangle$. For very small values of z_0 (large $\langle n\rangle$) the sum of the areas of the rectangles (total probability) equals the area under the curve, i.e. it is equal to unity. However, with increasing z_0 (with decreasing energy) these areas cannot, certainly, remain equal at each value of z_0. Our "numerical integration" becomes too rough.

The change of normalization with energy would mean the return of Ψ dependence on energy. Figure 2a approximately corresponds to the multiplicity distribution in PP interactions at $P_{lab}= 100$ GeV/c. The distribution of all charged particles is exactly the same; only the probabilities are redenoted according to (1): $P_0 \to P_2$, $P_1 \to P_4$ and so on. Thus, if arithmetic is valid, an

experimental check of eq. (2) cannot yield a positive result (at least up to ISR energies at a present-day accuracy of experimental data).

To test the hypothesis of similarity of multiplicity distributions, the concept of similarity for discrete functions is first to be defined. It should be consistent for $\langle n\rangle \simeq 1$ and return to the ordinary form (2) for $\langle n\rangle \gg 1$.

4. GENERALIZATION

An obvious generalization of the recipe of obtaining all multiplicity distributions from one universal function $\Psi(z)$ is shown in fig.2b where the partial probabilities P_n are merely equal to the area under the curve within the interval z_o. It is seen that the sum of probabilities is always equal to unity, and the figures a and b coincide for $z_o \to 0$. This can be expressed as [6]

$$P_n = \int_{nz_o}^{(n+1)z_o} \Psi(z)dz \ . \qquad (5)$$

Normalization conditions (3) and (4) for $\Psi(z)$ certainly remain. Now one can guess the function $\Psi(z)$ or obtain it from very high energies, when the approximate formula (2) is valid, and calculate all multiplicity distributions by eq. (5) substituting various scales z_o.

Let us introduce a continuous parameter $m = z/z_o$ which fills up gaps on the discrete n-axis in fig.1a and which we would have to introduce before obtaining formula (2) in order not to integrate over the discrete parameter n. Then eq. (5) can be rewritten in the form

$$P_n = \int_n^{n+1} P(m)dm \ , \qquad (6)$$

where

$$P(m) = 1/\langle m\rangle \ \Psi(m/\langle m\rangle) \qquad (7)$$

with

$$\langle m\rangle = \int_o^{\infty} mP(m)dm = 1/z_o \ . \qquad (8)$$

Thus, the discrete multiplicity distribution is presented as a histogram from the continuous function having KNO invariant properties.

One can say that the definition of the concept of similarity remained to be the definition for continuous functions. Only the recipe of obtaining the discrete distribution from the continuous function was changed. Instead of the inconsistent recipe actually used in (2)

$$P_n = P(m)|_{m=n} , \tag{9}$$

we deal now with the correct recipe (6).

Almost the same method of obtaining multiplicity distributions from the continuous function, which was not yet KNO invariant, was used in papers [7].

Eq. (5) can be presented in an integral form [6,8]

$$\sum_n^\infty P_k = \int_n^\infty P(m)dm = \int_{nz_o}^\infty \Psi(z)dz = \Phi(nz_o) , \tag{10}$$

where $\Phi(z) = \int_z^\infty \Psi(z)dz$ is a universal function normalized by the conditions

$$\Phi(0) = \int \Phi(z)dz = 1 , \tag{11}$$

which arises from the conditions (3) and (4). The partial probabilities are expressed through this function simpler than in (5)

$$P_n = \Phi(nz_o) - \Phi((n+1)z_o) . \tag{12}$$

In contradistinction to $\Psi(z)$, the function $\Phi(z)$ allows one to plot multiplicity distributions for a variety of energies on one curve according to (10) if the dependence of $\langle m\rangle = 1/z_o$ on energy or $\langle n\rangle$ is known (see [6,8] and also [9,10]).

5. APPROXIMATE CONSEQUENCES

For not very small values of $\langle n\rangle$, from (6) - (8) one can obtain approximately [6,8]

$$\langle m\rangle = \int mP(m)dm = \sum_n^{n+1} \int_n mP(m)dm \approx \sum_n (n+.5) \int_n^{n+1} P(m)dm = \sum_n (n+.5)P_n = \langle n\rangle + .5. \tag{13}$$

This is also seen from fig.2b since the area P_n lies between the abscissas n and n+1, therefore the abscissa n+.5 is to be assigned to the area P_n for an approximate calculation of the centre of the

continuous curve by the histogram. An accurate calculation shows that for very different functions $\Psi(z)$ this approximation ($\langle m\rangle = \langle n\rangle + .5$) works well already from $\langle n\rangle \geq .3$ which corresponds to $P_{lab} \simeq 4$ GeV/c in PP interactions.

For the central moments: $\mu_q = \int (m-\langle m\rangle)^q P(m)dm$ (continuous function) and $D_q^q = \Sigma (n-\langle n\rangle)^q P_n$ (discrete one) the result proves to be still simpler because the addition .5 to n and $\langle n\rangle$ cancels (the central moments are independent of the peak position on the abscissa axis)

$$\mu_q = \sum_n \int_n^{n+1} (m-\langle m\rangle)^q P(m)dm \approx \sum_n (n+.5-\langle n\rangle-.5)^q \int_n^{n+1} P(m)dm = D_q^q . \quad (14)$$

Therefore the known proportionality for continuous KNO invariant functions $\mu_q^{1/q} \propto \langle m\rangle$ leads to an approximate proportionality for discrete distributions

$$D_q \propto (\langle n\rangle + .5) , \quad (15)$$

which results in the Wroblewski relations [11] when passing to all charged particles in PP interactions according to (1)

$$D_q^{ch} \propto (\langle n_{ch}\rangle - 1). \quad (16)$$

For e^+e^- annihilation, eq.(15) yields $D_q^{ch} \propto (\langle n_{ch}\rangle + 1)$.

From (6), (7) and (13) we also get

$$P_n \approx P(m)|_{m=n+.5} = \frac{1}{\langle m\rangle} \Psi\left(\frac{n+.5}{\langle m\rangle}\right) \approx \frac{1}{\langle n\rangle + .5} \Psi\left(\frac{n+.5}{\langle n\rangle + .5}\right) , \quad (17)$$

which results in "improved KNO" [11] taking (1) into account:

$$P_{n_{ch}} = \frac{1}{\langle n_{ch}\rangle - 1} \Psi\left(\frac{n_{ch}-1}{\langle n_{ch}\rangle - 1}\right) . \quad (18)$$

6. COMPARISON WITH EXPERIMENT

As seen from fig.2b, if we have an experimental multiplicity distribution at some energy, we can obtain a distribution for a lower energy corresponding to z_o' which is twice as much. In this case $P_o' = P_o + P_1$; $P_1' = P_2 + P_3$; $P_2' = P_4 + P_5$ and so on. The same can be repeated for $z_o'' = 3z_o$: $P_n'' = P_{3n} + P_{3n+1} + P_{3n+2}$ and so on. A comparison of the points obtained by this method from ISR data with those at lower energies is made in figs. 3 and 4. One can see that they coincide down to the lowest energies. By the way, note that

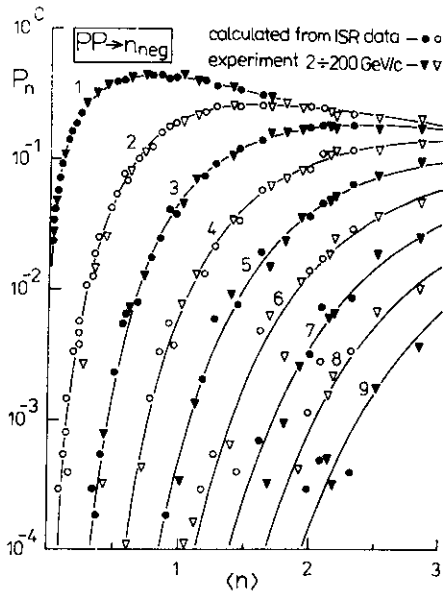

Fig. 3. Comparison of the experimental multiplicity distributions with the distributions calculated from those obtained for higher energies according to the recipe $P'_n=P_{2n}+P_{2n+1}$; $P''_n= P_{3n}+P_{3n+1}+P_{3n+2}$ and so on (see fig. 2b).

another recipe follows from formula (2): $P'_n= 2P_{2n}$; $P''_n= 3P_{3n}$ and so on, and the sums of the obtained probabilities cannot be exactly equal to 1. Figure 4 shows the Wroblewski straight lines and also the lower limits of values of D_q (D_q is minimum for a given value of $\langle n\rangle$ when only two neighbouring probabilities P_n are not equal to zero [12]).

The ratios $(\langle n\rangle+.5)/D_2$ and D_q/D_2 for PP inelastic interactions at $P_{lab}= 3\div2000$ GeV/c and for e^+e^- annihilation at $\sqrt{s}= 3\div35$ GeV are presented in figs. 5 and 6. Contrary to the commonly used variables $C_q= \langle n^q\rangle/\langle n\rangle^q$, these ratios should go fastly to the plateau with increasing energy as seen from eqs. (14) and (15). The presented errors are calculated under the

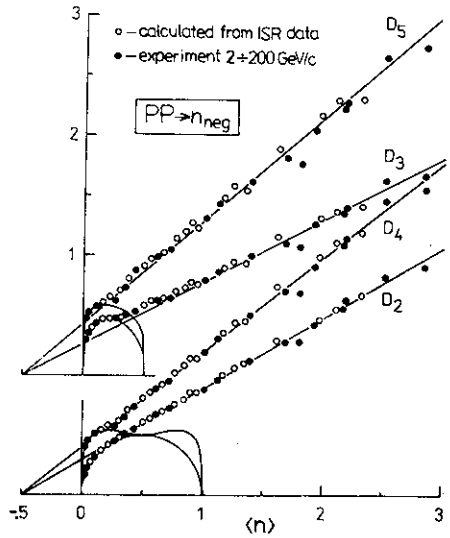

Fig. 4. $D_q = (\Sigma\,(n-\langle n\rangle)^q\,P_n)^{1/q}$ versus $\langle n\rangle$. The calculated points are obtained as in fig. 3.

assumption of normality and independence of the published errors of the cross sections. The curves are obtained according to formula (5) by substituting the functions

$$\Psi(z)_{pp} = a(z+.14)\,e^{-b(z+.14)^2}, \qquad (19)$$

$$\Psi(z)_{ee} = a(z-.17)^3\,e^{-b(z-.17)^2} \quad (\text{for } z \leq .17:\ \Psi=0). \qquad (20)$$

Here .14 and .17 are free parameters and the coefficients a and b obtained from (3) and (4) are respectively equal to 1.251 and .618 for PP and 13.16 and 2.565 for e^+e^-. The curves of fig. 3 are obtained in the same manner. Several different one-parameter functions, which describe the data well too, have been found for both cases (see also [8]). However, all of them contain $-z^2$ in the exponent [9]. The presented functions are chosen due to integration simplicity. They differ from those obtained in [13]

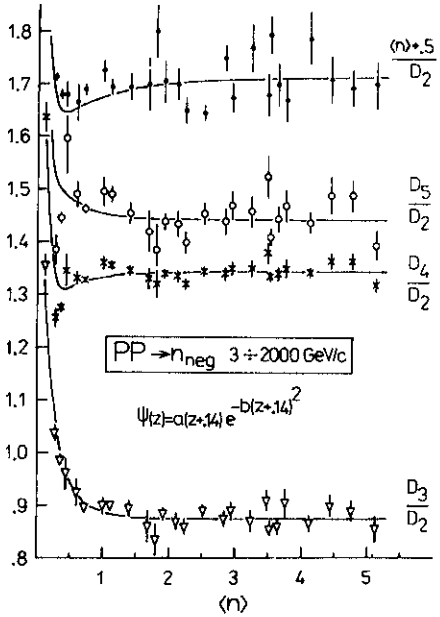

Fig.5. Ratios which should go fastly to the plateau with increasing energy if the "Accurate Multiplicity Scaling" is valid. The curves are obtained by formula (5) (fig.2b) with $\Psi(z)$ presented in the figure. The coefficients a and b calculated from the conditions (3), (4) are equal to 1.251 and .618, respectively.

only in shifts along the z-axis (-.14 and +.17). Calculating the curves for e^+e^-, P_o was set to zero since it was not measured experimentally which is essential only for the lowest energies though.

It is interesting that according to Polyakov's paper [14], where KNO scaling for e^+e^- annihilation was first predicted, the increase of $\langle n\rangle \alpha\ s^{1/4}$ should be obtained from such a fall of $\Psi(z)$ for large z (e^{-z^2}).

The Collider point at $\sqrt{s}$= 546 GeV is presented in figs. 7 and 8 along with other data. No data on inelastic interactions at 200 and 900 GeV have been published (only non single-diffractive).

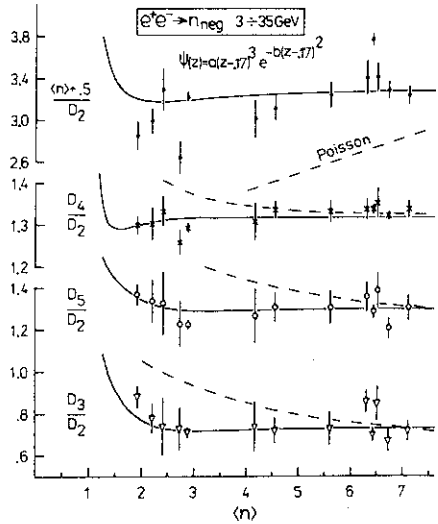

Fig.6. The same for e^+e^- interactions. For $z \leq .17$ $\Psi(z)=0$. The coefficients a and b are equal to 13.16 and 2.565, respectively.

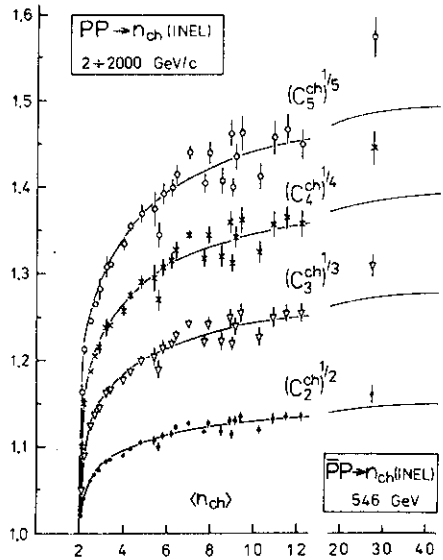

Fig.7. $(C_q^{ch})^{1/q} = \langle n_{ch}^q \rangle^{1/q} / \langle n_{ch} \rangle$ versus $\langle n_{ch} \rangle$. The curves are obtained from the scaling for negative particles as in fig.5 when passing to all charged particles according to (1).

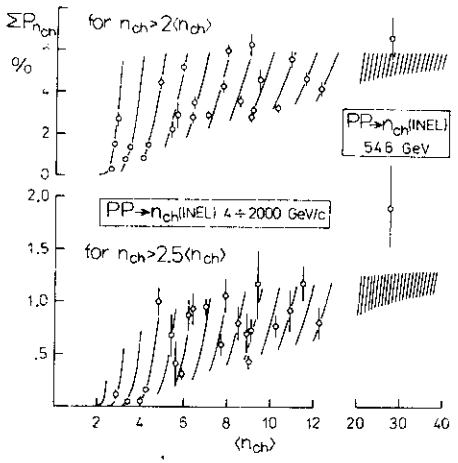

Fig.8. Percentage of events having $n_{ch} \geq 2\langle n_{ch}\rangle$ (or $2.5\langle n_{ch}\rangle$) versus $\langle n_{ch}\rangle$. The curves are obtained as in fig.7. Jumps of the function occurs when $2\langle n_{ch}\rangle$ ($2.5\langle n_{ch}\rangle$ becomes equal to an even integer since the next $P_{n_{ch}}$ does not already enter into this sum.

The quantities C_q in fig.7 are raised to the $1/q$ power for stretching the scale at small q. The curves are obtained using the same scaling function (19) for negative particles when passing to charged particles according to (1) (scaling (5) cannot be simultaneously performed for negative and charged particles in PP interactions due to shift $+2$ in (1)). Statistical and systematic errors for 546 GeV are added quadratically. An evidence for scaling violation is seen for the Collider energy (up to 3.5 errors for C_5).

Figure 8 shows the percentage of events with multiplicity which is 2 (2.5) times and more as large as the average one. Jumps of the curve occur with rising $\langle n_{ch}\rangle$ when $2\langle n_{ch}\rangle$ ($2.5\langle n_{ch}\rangle$) becomes equal to an even integer since the next partial probability $P_{n_{ch}}$ does not already enter into this sum. The errors for the Collider point are calculated taking into account the

errors of $\langle n_{ch} \rangle$: $2\langle n_{ch} \rangle = 55 \pm 1.3$. Therefore the sum should include events from $n_{ch} \geq 54$ at the lower bound of the error and from $n_{ch} \geq 58$ at the upper one. The same is for $2.5\langle n_{ch} \rangle = 68.8 \pm 1.7$ (68 and 72). Apparently, the height of the tail varies insignificantly at this variation of $\langle n_{ch} \rangle$.

ACKNOWLEGEMENTS

The author is grateful to S.A. Khorozov and R. Szwed for many fruitful discussions.

REFERENCES

1. e^+e^-: 3÷7 GeV: J.L. Siegrist et al.: Phys. Rev. D26, 969 (1982)
4÷9 GeV: B. Niczyporuk et al.: Z. Phys. C9, 1 (1981)
12÷35 GeV: W. Bartel et al.: Z. Phys. C20, 187 (1983)
14÷34 GeV: M. Althoff et al.: Z. Phys. C22, 307 (1984)
29 GeV: M. Derrick et al.: Phys. Rev. D34, 3304 (1986)
2. PP: 1.5÷2 GeV/c: F. Shimizu et al.: Nucl. Phys. A386,571 (1982)
2.23 GeV/c: A.M. Eisner et al.: Phys. Rev. 138B, 670 (1965)
2.81 GeV/c: E. Pickup et al.: Phys. Rev. 125, 2091 (1962)
4 GeV/c: L. Bodini et al.: Nuovo Cim. 58A, 475 (1968)
5.5 GeV/c: G. Alexander et al.: Phys. Rev. 154, 1284 (1967)
6.6 GeV/c: E.R. Gellert: LBL-749. Berkeley (1972)
10 GeV/c: S.P. Almeida et al.: Phys. Rev. 174, 1638 (1968)
12; 24 GeV/c: V. Blobel et al.: Nucl. Phys. B69, 454 (1974)
19 GeV/c: H. Boggild et al.: Nucl. Phys. B27, 285 (1971)
32 GeV/c: M.J.Bogolubsky et al.: Sov.J. Nucl.Phys.46,842 (1987)
35.7 GeV/c: I.V.Boguslavsky et al.: JINR 1-10134. Dubna (1976)
50 GeV/c: V.V. Ammosov et al.: Phys. Lett. 42B, 519 (1972)
60 GeV/c: C. Bromberg et al.: Phys. Rev. D15, 64 (1977)
69 GeV/c: V.V. Babintsev et al.: IHEP M-25. Serpukhov (1976)
100 GeV/c: W.M. Morse et al.: Phys. Rev. D15, 66 (1977)
102,405 GeV/c: C.Bromberg et al.: Phys.Rev.Lett. 31,1563 (1973)
147 GeV/c: D. Brick et al.: Phys. Rev. D25, 2794 (1982)

205 GeV/c: S. Barish et al.: Phys. Rev. D9, 2689 (1974)
250 GeV/c: M. Adamus et al.: Z. Phys. C32, 475 (1986)
300 GeV/c: A. Firestone et al.: Phys. Rev. D10, 2080 (1974)
360 GeV/c: J.L. Bailly et al.: Z. Phys. C23, 205 (1984)
400 GeV/c: R.D. Kass et al.: Phys. Rev. D20, 605 (1979)
800 GeV/c: R. Ammar et al.: Phys. Lett. 178B, 124 (1986)
$\sqrt{s}$=30÷60 GeV: A. Breakstone et al.: Phys. Rev. D30, 528 (1984)

3. $\bar{P}P$: $\sqrt{s}$=546 GeV: G.J. Alner et al.: Phys. Rep. 154, 247 (1987)
4. Z. Koba, H.B. Nielsen, P. Olesen: Nucl. Phys. B40, 317 (1972)
5. Z. Koba: Proc. 1973 CERN-JINR School of Phys., CERN 73-12 (1973)
6. A.I. Golokhvastov: Sov. J. Nucl. Phys. 27, 470 (1978); 30, 128 (1979)
   A.I. Golokhvastov: JINR E2-87-484. Dubna (1987)
7. G.V. Parry, P. Rotelli: IC/73/3. Triest (1973)
   G.V. Parry, P. Rotelli: Lett. Nuovo Cim. 7, 649 (1973)
8. R. Szwed, G. Wrochna: Z. Phys. C29, 255 (1985)
   R. Szwed: IFD/3/85; IFD/3/86; IFD/5/86; IFD/5/88. Warsaw
9. G. Bozoki et al.: Nuovo Cim. 64A, 881 (1969)
10. V.D. Aksinenko et al.: Nucl. Phys. A324, 266 (1979)
11. A. Wroblewski: Acta Phys. Pol. B4, 857 (1973)
    A.J. Buras, J. Dias De Deus, R. Møller: Phys. Lett. 47B, 251 (1973)
12. L.F. Zhirkov et al.: Sov. J. Nucl. Phys. 31, 102 (1980)
13. A. Buras, Z. Koba: Lett. Nuovo Cim. 6, 629 (1973)
    S. Barshay, Y. Yamaguchi: Phys. Lett. 51B, 376 (1974)
14. A.M. Polyakov: Sov. Phys. JETP 32, 296 (1971)

Received by Publishing Department
on May 17, 1989.